

DNA bending by photolyase in specific and non-specific complexes studied by atomic force microscopy

John van Noort, Francesco Orsini, Andre Eker¹, Claire Wyman¹, Bart de Grooth* and Jan Greve

Applied Optics Group, Department of Applied Physics, University of Twente, PO Box 217, 7500 AE Enschede, The Netherlands and ¹Department of Cell Biology and Genetics, Medical Genetics Centre, Erasmus University, PO Box 1738, 3000 DR Rotterdam, The Netherlands

Received May 14, 1999; Revised and Accepted August 12, 1999

ABSTRACT

Specific and non-specific complexes of DNA and photolyase are visualised by atomic force microscopy. As a substrate for photolyase a 1150 bp DNA restriction fragment was UV-irradiated to produce damaged sites at random positions. Comparison with a 735 bp undamaged DNA fragment made it possible to separate populations of specific and non-specific photolyase complexes on the 1150 bp fragment, relieving the need for highly defined substrates. Thus it was possible to compare DNA bending for specific and non-specific interactions. Non-specific complexes show no significant bending but increased rigidity compared to naked DNA, whereas specific complexes show DNA bending of on average 36° and higher flexibility. A model obtained by docking shows that photolyase can accommodate a 36° bent DNA in the vicinity of the active site.

INTRODUCTION

Many genome transactions require proteins to recognise and act at specific sequences or structures in DNA. Specific site recognition often requires or results in changes in DNA conformation. Analysis of DNA deformation within a specific protein–DNA complex can yield important information on the mechanism of site recognition. The flexibility of DNA complexed to protein has been suggested to play a role in site recognition and can also be expected to influence downstream biochemical reactions (1). Within the resolution limits of the technique, atomic force microscopy (AFM) studies of protein–DNA complexes yield valuable information on the global arrangement of proteins and DNA, as well as the variety and distribution of different structures in a population.

Protein-induced DNA bending can be easily measured by AFM. Where comparison is possible, AFM-determined bending angles agree well with those determined by X-ray crystallography and gel band shift methods (2). However, among these methods AFM uniquely reveals the flexibility of protein–DNA complexes through analysis of the distribution of the DNA bending angles.

Photolyase, a 55 kDa protein, uses near-UV or visible light (300–500 nm) to reverse UV-induced dimerisation of two adjacent pyrimidine bases in DNA. Photolyase binds to pyrimidine dimers with high specificity and affinity independent of the surrounding DNA sequence (3). Based on the crystal structure of photolyase, Park *et al.* (4) speculated about structural features involved in binding to and repair of DNA. However, the three-dimensional structure of the photolyase–DNA complex has not yet been determined, leaving the detailed mechanism of substrate recognition and specific binding to UV-induced pyrimidine dimers in DNA largely unknown.

In this study data will be presented on the conformation of DNA when photolyase is bound at specific and non-specific sites. In our experiments UV-irradiated fragments that contain randomly located damaged sites can be distinguished from fragments that had not been irradiated, based on their contour length. Thus, populations of specific and non-specific interactions can be discriminated, relieving the need for a highly defined substrate necessary for other techniques. A direct comparison is made between the bending and flexibility of specific complexes and non-specific complexes and naked DNA.

MATERIALS AND METHODS

Sample preparation

DNA fragments used for photolyase binding were released from pET-XPB (5) by *NcoI* digestion. The digested DNA was separated on an agarose gel and the 1150 and 735 bp fragments, from the cDNA sequence of the human XPB gene, were isolated by electroelution. DNA photolyase from *Anacystis nidulans* was purified to apparent homogeneity as described previously (6). As a substrate for photolyase 1150 bp DNA was irradiated with ~3800 J/m² UV (254 nm), introducing damage, mainly pyrimidine dimers, at random sites. Reaction mixtures with a final volume of 10 µl contained 8.0 µg/ml of the damaged fragment, 4.8 µg/ml of an undamaged 735 bp restriction fragment and 0.45 µg/ml photolyase in 100 mM NaCl, 4 mM HEPES, pH 6.5, 5 mM MgCl₂, 1 mM β-mercaptoethanol. After 10 min the reaction mixture was diluted 10 times in deposition buffer, consisting of 20 mM HEPES, pH 6.5, 5 mM MgCl₂, 1 mM β-mercaptoethanol. Within 1 min a 5 µl drop was pipetted onto a freshly cleaved mica disk and after ~30 s rinsed with water and blown dry with nitrogen gas. To prevent photorepair before immobilisation, all sample manipulation was performed in the dark.

*To whom correspondence should be addressed. Tel: +31 534 89 3157; Fax: +31 534 89 1105; Email: b.g.degrooth@tn.utwente.nl

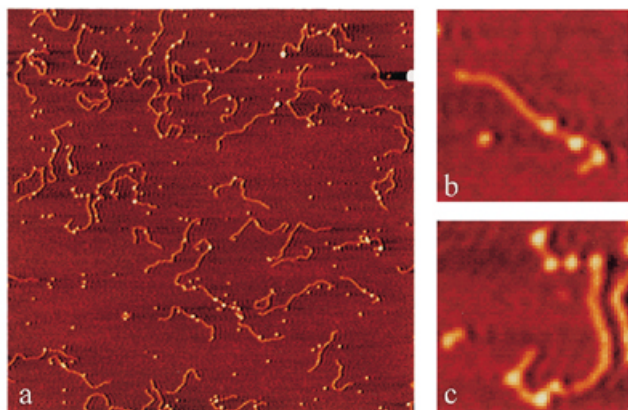


Figure 1. (a) An AFM image of a reaction mixture of photolyase and 735 and 1150 bp restriction fragments; scan area $2 \times 2 \mu\text{m}^2$, height range 4 nm. The 1150 bp restriction fragment was irradiated with UV before deposition. (b) Software zoom of a 735 bp DNA fragment with photolyase. (c) Software zoom of a 1150 bp DNA fragment with photolyase; scan area $250 \times 250 \text{ nm}^2$. The latter fragment is clearly longer and contains more photolyase molecules.

AFM set-up

Triangular Si_3N_4 cantilevers purchased from Park Scientific instruments (Sunnyvale, CA), with a spring constant of 0.5 N/m and a resonance frequency of 110 kHz, were used in a home built AFM (7). Images with a scan area of $2 \times 2 \mu\text{m}^2$, 512×512 pixels, were acquired in tapping mode, using a free peak-to-peak amplitude of 200 nm, an amplitude set-point of 180 nm and a pixel rate of 6 kHz.

Image processing and data analysis

AFM data were processed using the Interactive Data Language (RSI, Austin, CO) in a self-written software package. Standard image processing consisted of line subtraction by fitting of a second order polynomial to each line in the image. The contours of DNA molecules were hand traced by selection of 2–8 points along a DNA strand, using an algorithm similar to that described by Rivetti *et al.* (8). Proteins were manually selected. Because tip-sample convolution limits the resolution of AFM images, the DNA strand can only be resolved ~ 10 nm from the centre of the protein. Bending angles were determined by evaluating the angle between the centre of the protein and a point 15 nm upstream and downstream on the DNA, as shown in Figure 1. The measured bending angles are expected to show a Gaussian distribution (2). Because we only measure the smallest angle Θ and because angle distributions are truncated at 0° (9), the distribution was fitted with:

$$P(\Theta) = Ae^{-\frac{(\Theta - [\Theta])^2}{2\sigma^2}} + Ae^{-\frac{(\Theta + [\Theta])^2}{2\sigma^2}} \quad 1$$

where A is a normalisation constant and σ the standard deviation.

RESULTS

A typical AFM image of photolyase–DNA complexes is shown in Figure 1a. Photolyase has a diameter of ~ 5 nm and

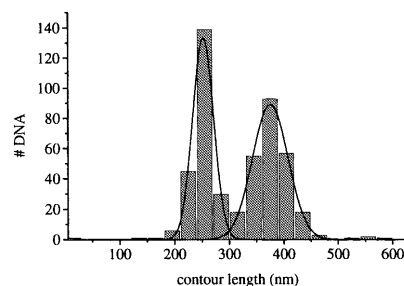


Figure 2. Measured contour length distribution of a mixture of 735 and 1150 bp restriction fragments. Solid lines show Gaussian fits of two peaks, resulting in 252 ± 36 nm for the smaller fragment and 366 ± 64 nm for the longer fragment.

appears as 3 nm high globular structures on DNA molecules. The height of tapping mode AFM images is not very accurate, depending on tip–surface interaction and feedback settings (10), which explains the discrepancy between theoretical and observed height of the DNA and the protein. Photolyase molecules are observed on both 1150 and 735 bp restriction fragments. Figure 1b shows a zoom of an undamaged 735 bp molecule, while Figure 1c shows a UV-irradiated 1150 bp DNA fragment. The latter fragment is longer and contains more photolyase molecules.

The contour length of all DNA molecules was determined by hand tracing and the resulting contour length distribution is plotted in Figure 2. Two peaks at 252 and 366 nm, corresponding to 735 and 1150 bp, are clearly resolved. Thus UV-damaged DNA fragments can be clearly distinguished from undamaged DNA fragments based on their contour lengths. For the rest of this analysis fragments with measured contour lengths < 300 nm were classified as non-damaged, while fragments > 330 nm were classified as UV-irradiated.

The numbers of photolyase–DNA complexes on both DNA fragments are listed in Table 1. We expect the same number of non-specific complexes per kb on both damaged and non-damaged fragments. This was confirmed by repeating the experiment with restriction fragments that were not exposed to UV radiation. In this experiment no significant difference was found between the number of complexes per kb, which excludes sequence-specific and length-dependent effects.

Thus 78% of the photolyase molecules bound to UV-irradiated fragments are non-specific complexes, resulting in an average of 0.7 specific complexes per 1150 bp DNA fragment. Assuming a complex dissociation constant $K_d \approx 10^{-8}$ (3), half of the damaged sites are expected to be occupied by photolyase in the reaction buffer and the number of damaged sites can be estimated to be ~ 2 per 1150 bp DNA. This number is approximately 10 times less than we expected based on the UV dose the DNA was exposed to. However, in the dilution step that is necessary for immobilisation of DNA on mica, specific complexes may have dissociated, causing an underestimation of the number of damaged sites (see Discussion). Because the 735 bp fragment is used as an internal reference, our characterisation of specifically bound photolyase protein on damaged DNA will not be influenced

Table 1. Summary of the number of photolyase–DNA complexes found on undamaged and UV-damaged DNA fragments

DNA size	UV	No. of DNA molecules	No. of photolyase–DNA complexes	No. of photolyase–DNA complexes/DNA molecule	No. of photolyase–DNA complexes/kb
735 bp	–	246	172	1.4	1.94 ± 0.12
1150 bp	–	287	134	2.1	1.86 ± 0.11
735 bp	–	396	220	1.8	2.45 ± 0.07
1150 bp	+	1544	432	3.6	3.11 ± 0.02

by the likelihood that not all damaged DNA sites are occupied by photolyase.

In order to obtain reliable data on the conformation of a protein–DNA complex it is important that during deposition the DNA is able to equilibrate on the mica deposition surface (2). This condition was checked by measurement of the persistence length of undamaged DNA molecules that did not contain any photolyase molecules. DNA molecules that can diffuse over the surface are expected to have a persistence length of 53 nm (independent of the actual length of the DNA), which is also found for DNA in solution (11). For DNA molecules that cannot diffuse over the surface a much smaller persistence length has been measured (8). Using a method based on end-to-end distance measurements (8), we found a persistence length of 56 nm measured for 45 undamaged DNA fragments. This shows that under the conditions used, DNA is able to diffuse freely to find the energetically most favourable conformation. Thus, immobilisation of DNA–photolyase complexes is not expected to have perturbed protein-induced bending of DNA.

The bending angle of all the complexes located >15 nm from a DNA end was measured. Distributions of bending angles on both fragments are shown in Figure 3a and b. On 735 bp fragments all complexes are non-specific photolyase–DNA interactions. When fitted to equation 1 a bending angle of $0 \pm 18^\circ$ was measured for these non-specific complexes.

On 1150 bp fragments a much broader distribution of bending angles is measured, originating from both specific and non-specific interactions. The bending angle distribution of specific complexes can be obtained by subtraction of the contribution of non-specific complexes from the angle distribution on 1150 bp DNA fragments. In this experiment 78% of the complexes on 1150 bp DNA fragments are non-specific. Thus the fitted distribution of non-specific complexes was divided by the number of complexes that contributed to Figure 3a. This distribution was multiplied by 0.78 times the number of complexes contributing to Figure 3b and subtracted from it. The results represent the bending angle distribution of specific photolyase–DNA complexes and are plotted in Figure 3c. The fit of this distribution reveals an average bending angle of $36 \pm 30^\circ$.

For comparison, the bending angle of DNA at random positions at least 50 nm away from a complexed photolyase was also measured (Fig. 3d), resulting in an angle of $0 \pm 24^\circ$. As expected, no bending of DNA was measured.

The standard deviation of the bending angle distribution does not represent the error in the measurement, but is proportional to the flexibility. The flexibility of a DNA molecule is characterised by its persistence length and the standard deviation of the bending angle can be related to this persistence length. The

standard deviation of the angle distribution of unbound DNA was 24° , which is slightly more than the 21° that would be expected based on the persistence length found by measurement of the end-to-end distance.

For protein–DNA complexes the standard deviation of the bending angle reflects the flexibility of the protein–DNA complex. However, because of resolution limitations, we could only measure the bending angle over 30 nm, a length longer than photolyase can physically cover. The flexibility of the DNA extending from the protein will add to the standard deviation, resulting in a broader angle distribution than that of the complex itself. The measured average angle, however, is not affected. The standard deviation of the bending angle of protein–DNA complexes can be compared with that of unbound DNA. The results of the bending angle measurements are summarised in Table 2. Both the decrease in standard deviation of the non-specific and the increase in the standard deviation of the specific complex relative to naked DNA are statistically relevant with a confidence level of >99.9%. Thus in non-specific complexes photolyase decreases the flexibility of DNA, but in specific complexes DNA appears more flexible than unbound DNA.

Table 2. Summary of the bending angle distribution, as fitted to equation 1, for specific and non-specific photolyase–DNA complexes and for naked DNA

	Θ (deg)	σ (deg)	n
Non-specific complex	0	18	321
Specific complex	36	30	328
Naked DNA	0	24	3656

Θ , average angle; σ , standard deviation; n , number of measurements.

DISCUSSION

We have visualised photolyase–DNA complexes with AFM in air and analysed the global conformation of these complexes. By comparing damaged with undamaged DNA it was possible to discriminate between distributions of specific and non-specific interactions using DNA fragments of different size. It is shown that DNA in the reported experiments was able to equilibrate on the surface, which points to weak DNA surface interactions. Thus the deposition process itself can be expected to have little influence on the number of interactions and the conformation of photolyase–DNA complexes.

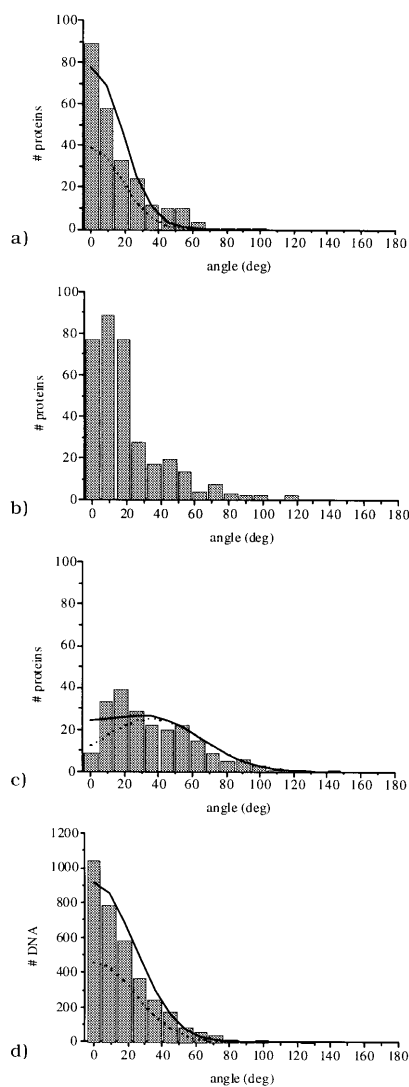


Figure 3. Bending angle distributions of photolyase–DNA complexes and naked DNA. (a) Non-specific complexes on 735 bp DNA. (b) Mixture of specific and non-specific complexes on 1150 bp DNA. (c) Specific complexes on 1150 bp DNA obtained by subtraction from (b) of the distribution obtained from (a), corrected for size and number of complexes. (d) A reference angle distribution of DNA on random positions on the DNA strand. The solid line represents a fit using equation 1. The dotted line represents a Gaussian distribution using the fitted average angle and standard deviation of equation 1.

Recently, a number of studies on the structure of *Escherichia coli* photolyase and its interaction with DNA have been reported in the literature (3,4,11,12). Because of the large degree of similarity with *A.nidulans* photolyase (13), we relate some of these results to the data in this paper. In contrast to Sancar *et al.* (14), who imaged individual *E.coli* photolyase–DNA complexes by electron microscopy, we observed a significant number of non-specific complexes. The difference may be explained by the different preparation protocol. For optimal measurement the AFM image should represent the equilibrium state of complex formation. The association rate constant for

specific complexes is in the range 10^6 – 10^7 $M^{-1} s^{-1}$ (3), thus a 10 min incubation should be enough to reach equilibrium. Before DNA immobilisation on mica, the reaction mixture was diluted 10 times in a low salt deposition buffer. In general, low salt conditions enhance non-specific complexes and dilution in this buffer may have increased the number of non-specific complexes. The dissociation rate of specific complexes was estimated to be 2×10^{-2} to 6×10^{-4} s^{-1} for *E.coli* photolyase (14), but can range up to $0.48 s^{-1}$ for *Streptomyces griseus* photolyase (15) and it may also vary with different buffer conditions. When the lifetime of the complexes is in the range of the time necessary for dilution and deposition, dissociation of specific complexes is very likely and may account for the differences. Indeed, for *E.coli* RNA polymerase it has been shown experimentally that the number of specific complexes decreases when rinsing protein–DNA samples thoroughly before drying (9). The number of specific interactions and therefore the estimated number of damaged sites on UV-irradiated DNA fragments will be underestimated if dissociation during sample preparation is not taken into account.

In non-specific complexes photolyase does not bend DNA. This observation is in contrast to Cro protein (21) and other sequence-specific DNA binding proteins that have been studied (2), which bend DNA when bound to specific and non-specific sequences. DNA bound by protein is expected to have less conformational freedom and hence to be more rigid than naked DNA. The narrower bending angle distribution and thus increased rigidity of non-specific complexes close contact between DNA and photolyase over several nanometers. It is interesting to compare this result with the reaction mechanism proposed by Park *et al.* (3) when they presented the crystal structure of photolyase. DNA is suggested to bind to the flat surface of the helical domain with the phosphate backbone of one strand following a trace of positive electrostatic potential that runs across this surface. Consistent with this model, the measured decrease in standard deviation of 6° indicates that the DNA molecule is rigid over a range of about the size of a photolyase molecule. A longer interaction range would require DNA to be wrapped around photolyase, introducing a bend of the DNA, which is not observed.

Usually, the extent of DNA covered by a protein is studied using footprinting techniques. Footprinting, however, cannot be used for non-specific complexes as no unique binding site can be defined. Based on AFM data we suggest that photolyase binds to DNA over several nanometers, without distorting the structure of DNA. From this data, it is tempting to suggest a mechanism of photolyase diffusion over DNA through the groove in the protein, to find damaged sites. AFM measurements in liquid indeed show one-dimensional movement along DNA strands (23).

Recently the structure of a duplex DNA dodecamer containing a cyclobutane thymine dimer was determined by NMR (24). It is shown that a thymine dimer introduces a small bend of 7° in the DNA molecule. Such small distortions in the DNA structure are not likely to be distinguished using AFM. Indeed, in the experiments no obvious changes in conformation, like sharp kinks, were observed in the 1150 bp fragments.

We showed that on average photolyase bends DNA by 36° when bound to damaged sites. This may include a slight intrinsic bend of the damaged site, but is likely to be mainly protein induced.

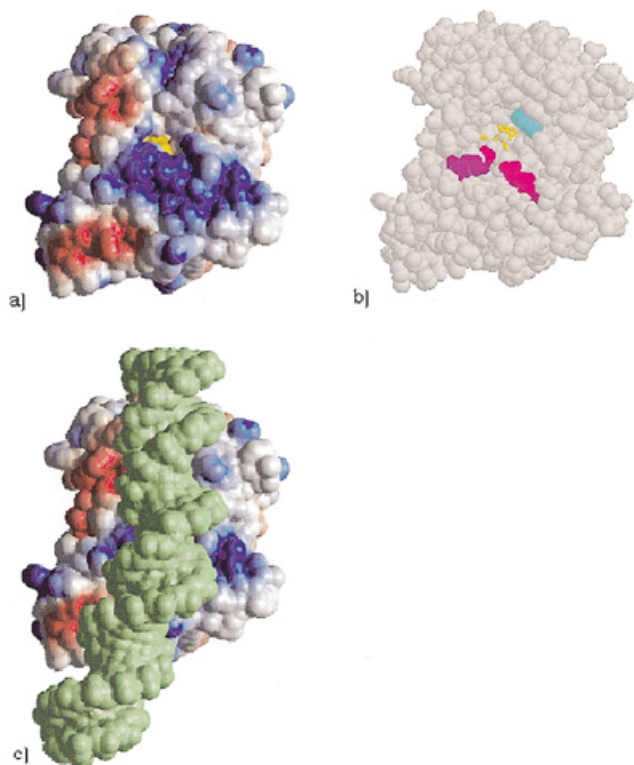


Figure 4. Putative model of the photolyase–substrate complex. (a) Solvent accessible surface (MOLMOL; 16) of *A.nidulans* photolyase coloured according to the calculated electrostatic potential (blue positive, white neutral and red negative). The central FAD chromophore is coloured yellow. (b) Space filled representation (RASMOL; 17) showing conserved arginine (magenta), lysine (purple) and tryptophan (cyan) residues which are involved in substrate binding in *S.cerevisiae* (18,12) and *E.coli* (19); FAD is coloured yellow. (c) Model of the photolyase–substrate complex. A 30mer DNA (green) was bent 36° (DIAMOD; 20) and docked onto *A.nidulans* photolyase by low resolution geometrical docking (GRAMM; 21).

Our observation that DNA is significantly bent by photolyase in specific complexes is consistent with a structure where the damaged bases are flipped out of the DNA helix into a pocket in the protein. So far, two examples of DNA repair enzymes have been reported in which bases are flipped out of the DNA helix when a complex is formed. The damaged nucleotide acted on by human 3-methyladenine DNA glycosylase is isolated out of the DNA helix, which is bent by 22° at this point (25). T4 endonuclease V, which cuts a DNA strand next to pyrimidine dimers, also binds an extra helical base, but in this case a nucleotide from the strand opposite to the damaged strand is flipped out of the helix. Damaged DNA in complex with T4 endonuclease V is bent by 60° (26). For photolyase, flipping out of the pyrimidine dimer in the substrate complex has been suggested (3).

In specific complexes of *E.coli* photolyase four to five phosphates on the damaged strand around the dimer are in contact with the protein in a groove of positive electrostatic charge, as measured by footprinting (11) and site-specific mutation

experiments (12). In the centre of this groove is a hole with the right dimensions and polarity to enclose a pyrimidine dimer that has flipped out of the helix, enabling the dimer to approach the FAD chromophore close enough to allow electron transfer necessary for the dimer splitting reaction (3). A comparable groove is present in *A.nidulans* photolyase (see Fig. 4a). Docking simulations, using a 30mer DNA with 36° bend angle indicate that the kinked DNA fits into this groove with the kink in the immediate vicinity of the FAD-containing active site (see Fig. 4c). Both non-bent and 45° bent DNA resulted in a poorer fit. Global comparison with the electrostatic surface potential of *A.nidulans* photolyase (Fig. 4a) and comparison with the location of amino acids that are known to play an important role in substrate recognition (Fig. 4b) show that in this respect a good fit is also obtained. However, the model is based on static geometrical docking only and interactions with a flipped pyrimidine dimer have not been taken into account. At present we have no direct evidence that DNA actually follows this path on the protein surface. Clarification of the exact structure must await high resolution structural determination of the damaged DNA–photolyase complex.

The increased flexibility of DNA that we observe in specific complexes was initially puzzling, as one would expect that bound protein would restrict the conformational freedom of DNA. However, this result could be accounted for by the model with the thymine dimer flipped out of the helix. It is difficult to predict the precise structural consequences this would have for the DNA, but it obviously necessitates leaving two unpaired bases on the opposite strand. Recently Rivetti *et al.* (27) showed that even a single base gap in a double-stranded DNA molecule greatly increases the flexibility, characterised by a decrease in persistence length from 53 to 1.7 nm. Though unpaired bases are not the same as a gap, we may expect some increase in flexibility of the DNA. Extra flexibility due to unpaired bases would be evident, even in the complex.

CONCLUSIONS

By using undamaged and damaged DNA fragments with different lengths, populations of specific and non-specific protein–DNA complexes can easily be discriminated. While other techniques require highly specific substrates for the study of protein–DNA interactions, we present an approach using AFM that is far less demanding for sample preparation. In addition, it is possible to compare the structure of proteins bound to specific and non-specific sites in the same sample and thus formed under identical conditions. We have shown that photolyase induces DNA bending only when bound to specific sites, whereas non-specific complexes do not bend DNA. At non-specific interaction sites DNA is shown to be more rigid than unbound DNA, while in specific complexes DNA appears more flexible.

REFERENCES

- Schepartz, A. (1995) *Science*, **269**, 989–990.
- Bustamante, C. and Rivetti, C. (1996) *Annu. Rev. Biophys. Biomol. Struct.*, **25**, 395–429.
- Sancar, A. (1994) *Biochemistry*, **33**, 2–9.
- Park, H.-W., Kim, S.-T., Sancar, A. and Deisenhofer, J. (1995) *Science*, **268**, 1866–1872.
- Weeda, G., Van Ham, R.C.A., Vermuelen, W., Bootsma, D., Van der Eb, A.J. and Hoeijmakers, J.H.J. (1990) *Cell*, **62**, 777–791.

6. Eker,A.P.M., Kooiman,P., Hessels,J.K.C. and Yasui,A. (1990) *J. Biol. Chem.*, **265**, 809–815.
7. Van der Werf,K.O., Putman,C.A., de Grooth,B.G., Segerink,F.B., Schipper,E.H., van Hulst,N.F. and Greve,J. (1993) *Rev. Sci. Instrum.*, **64**, 2892–2897.
8. Rivetti,C., Guthold,M. and Bustamante,C. (1996) *J. Mol. Biol.*, **264**, 919–932.
9. Schulz,A., Mücke,N., Langowski,J. and Rippe,K. (1998) *J. Mol. Biol.*, **283**, 821–836.
10. Van Noort,S.J.T., van der Werf,K.O., de Grooth,B.G., van Hulst,N.F. and Greve,J. (1997) *Ultramicroscopy*, **69**, 117–127.
11. Husain,I., Sancar,G.B., Holbrook,S.R. and Sancar,A. (1987) *J. Biol. Chem.*, **262**, 13188–13197.
12. Van de Berg,B.J. and Sancar,G.B. (1998) *J. Biol. Chem.*, **273**, 20276–20284.
13. Tamada,T., Kitadokoro,K., Higuchi,Y., Inaka,K., Yasui,A., de Ruiter,P.E., Eker,A.P.M. and Miki,K. (1997) *Nature Struct. Biol.*, **4**, 887–891.
14. Sancar,G.B., Smith,F.W., Reid,R., Payne,G. Levy,M. and Sancar,A. (1987) *J. Biol. Chem.*, **262**, 478–485.
15. Eker,A.P.M., Hessels,J.K.C. and Dekker,R.H. (1986) *Photochem. Photobiol.*, **44**, 197–205.
16. Koradi,R., Billeter,M. and Wüthrich,K. (1996) *J. Mol. Graph.*, **14**, 51–55.
17. Sayle,R.A. and Milner-White,E.J. (1995) *Trends Biochem. Sci.*, **20**, 374.
18. Bear,M.E. and Sancar,G.B. (1993) *J. Biol. Chem.*, **268**, 16717–16724.
19. Li,Y.F. and Sancar,A. (1991) *Biochemistry*, **29**, 5689–5705.
20. Dlakic,M. and Harrington,R.E. (1998) *Bioinformatics*, **14**, 326–331.
21. Vakser,I.A. (1996) *Biopolymers*, **39**, 455–464.
22. Erie,D.A., Yang,G., Schultz,H.C. and Bustamante,C. (1994) *Science*, **266**, 1562–1566.
23. Van Noort,S.J.T., van der Werf,K.O., Eker,A.P.M., Wyman,C., de Grooth,B.G., van Hulst,N.F. and Greve,J. (1998) *Biophys. J.*, **74**, 2840–2849.
24. McAteer,K., Jing,Y., Kao,J., Taylor,J.-S. and Kennedy,M.A. (1998) *J. Mol. Biol.*, **282**, 1013–1032.
25. Lau,A.Y., Schäfer,O.D., Samson,L., Verdine,G.L. and Ellenberger,T. (1998) *Cell*, **95**, 249–258.
26. Vassilyev,D.G., Kashiwagi,T., Mikami,Y., Ariyoshi,M., Iwai,S., Ohtsuka,E. and Morikawa,K. (1995) *Cell*, **83**, 773–782.
27. Rivetti,C., Walker,C. and Bustamante,C. (1998) *J. Mol. Biol.*, **280**, 41–59.